MARS SAMPLE RETURN: MISSION ANALYSIS FOR AN ESA EARTH RETURN ORBITER

Eric Joffre[(1)], *Uwe Derz*[(1)], *Marie-Claire Perkinson*[(1)]
Jakob Huesing[(2)], *Friederike Beyer*[(2)], *Jose-Manuel Sanchez Perez*[(3)]

(1) Airbus, Gunnels Wood Road, Stevenage SG1 2AS, UK
(2) ESA, Keplerlaan 1, PO Box 299, NL-2200 AG Noordwijk, The Netherlands
(3) ESA, Robert-Bosch-Straße 5, 64293 Darmstadt, Germany

ABSTRACT

Bi-lateral discussions between NASA and the European Space Agency identified the orbiter element as a promising European-led contribution to a future international Mars Sample Return campaign. Airbus recently completed the Mars Sample Return Architecture Assessment Study on behalf of ESA, with the objective to identify and quantify candidate mission architectures. The paper describes the mission analysis that has been conducted to support preliminary system design, launch mass estimation and mission timeline for the architectures investigated. It includes the optimisation of interplanetary transfers, Mars operations including aerobraking and rendezvous, up to Earth re-entry conditions.

1. INTRODUCTION

Between July and November 2017, Airbus Defence and Space conducted the *Mars Sample Return Architecture Assessment Study* (MSR-AA) on behalf of the European Space Agency, with the objective to: quantify mission architectures for an international Mars Sample Return (MSR) campaign, identify design envelopes for the candidate architectures (specifically addressing the elements that could be contributed by ESA), support identification and selection of ESA contributions to the campaign, and provide inputs to the technology development planning.

Bi-lateral discussions between ESA and NASA rapidly identified the orbiter element as a promising European-led contribution, which therefore became the primary focus of the study. In order to support the architecture trade-off and selection, a set of constraints and requirements were defined by the Agency in the early stages of the study: these covered aspects such as timeline requirements, target Launch Vehicles, payload masses and communication relay provision in Mars orbit. Based on these requirements, and also using Airbus heritage in previous MSR activities including the *Mars Sample Return Orbiter* (MSRO) Phase A study conducted for ESA in 2011-2012, a set of architecture options were investigated by Airbus as candidate solutions to the challenging mission requirements, addressing critical design drivers such as the Launch Vehicle selection, propulsion type, number of stages and point(s) of stage separation, as well as the use of aerobraking.

After presenting the mission overview and driving requirements for the MSR-AA study, the paper will describe the mission analysis activities conducted in support of this architecture assessment.

2. MISSION OVERVIEW AND KEY DRIVING REQUIREMENTS

2.1. Mars Sample Return Campaign Overview (credits: ESA)

The MSR campaign is comprised of three missions to be separately launched in the 2020s. These missions will work together to achieve the objective of returning to Earth a set of rigorously documented Mars atmospheric, soil, and rock core samples before the end of 2029. An overview of the campaign is shown in Figure 1.

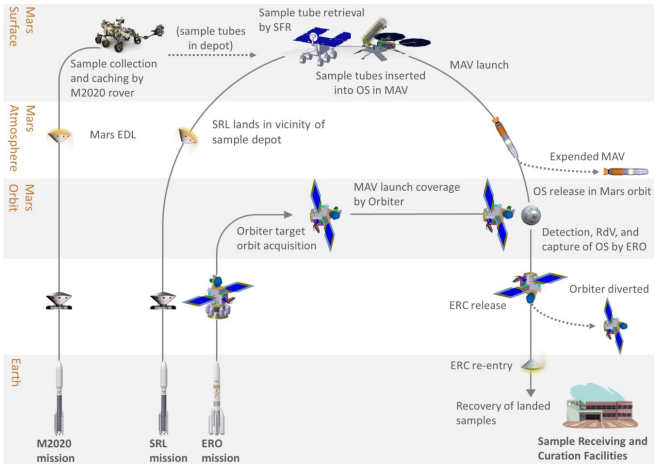

Fig. 1. MSR campaign overview (credits: ESA)

NASA's Mars 2020 mission, based on MSL heritage, will provide the first MSR mission, launching in mid-2020 and

landing the subsequent year. The rover's scientific payload includes equipment for performing the acquisition of target samples and caching them into specialised sample tubes. The mission will document the field context for each sample based on in situ observations. Once cached, the sample tubes will be placed in one or more depots for collection by the subsequent MSR surface mission. The landing site for this mission has been the subject of an extensive series of workshops, the last of which was held in February 2017. Three candidate landing sites currently remain: Jezero Crater, North East Syrtis, and Columbia Hills.

The Sample Return Lander (SRL) mission will launch in 2026. This mission is comprised of three elements; a surface platform, a Sample Fetch Rover (SFR), and a Mars Ascent Vehicle (MAV). The surface platform will touchdown in the near vicinity of the pre-designated sample tube depot. Once deployed to the surface, the SFR will traverse toward the depot(s), collect the sample tubes, and return to the lander platform. The sample tubes will then be transferred by the SRL robotic arm into an Orbiting Sample (OS) containment element, and loaded on-board the MAV. The MAV launches the OS into Mars orbit, where it is to be captured by the ERO mission.

The Earth Return Orbiter (ERO) mission will also launch in 2026. The spacecraft features a payload composed of two elements; a sample handling payload to perform the capture, and bio-sealing of the OS, and an Earth Re-entry Capsule (ERC). Following a transfer to Mars, the spacecraft will arrive at the expected OS target orbit in time to provide coverage of the MAV launch placing the OS into Mars orbit. The ERO will then detect, rendezvous with, and capture the OS, before biosealing it and transferring it safely to the ERC. After returning to Earth, ERO will release the ERC on an Earth entry trajectory before performing an Earth avoidance manoeuvre itself. After touchdown on Earth, the samples are transferred to a dedicated sample receiving and curation facility.

2.2. ERO Mission Architecture Key Driving Requirements

As presented in the introduction, the focus of the MSR-AA study has been on the assessment of potential mission architectures for the orbiter (ERO) mission, as a candidate ESA contribution to the MSR campaign. At the beginning of the study, a number of mission requirements have been provided by the Agency for the architecture assessment: a small subset of the most critical requirements relevant to the mission analysis activities is reported below for reference.

- The mission shall be launched by an Ariane 6 from Kourou (baseline).
- The mission shall be designed for a launch in 2026 as a baseline, with 2028 as back-up.
- The mission design shall be compatible with an Orbiting Sample (OS) container arrival no earlier than early 2028 (for a 2026 lander launch) or mid 2030 (for a 2028 lander launch).
- The mission shall provide communications relay functions to the surface mission, covering the Entry, Descent and Landing (EDL) of the SRL, the surface operations until MAV launch and the MAV launch phase. *NB The EDL coverage constraint was later reformulated as a mission design goal, rather than a strict requirement.*
- The mission shall be compatible with a reference OS orbit with a semi-major axis corresponding to 343 $\pm$ 30 km altitude above the surface of Mars, nominally circular (e $\leq$ 0.02).
- The mission should return the samples by 2030.

One of the main challenges of the ERO mission is linked to the very tight timeline imposed by the target launch date and the latest acceptable date for the return of the samples back to Earth. The mission architecture assessment has been conducted by selecting interplanetary (outbound and inbound) transfers compatible with those boundary conditions, but also arriving at Mars early enough for the surface mission coverage and leaving enough time for the subsequent rendezvous operations.

The baseline Launch Vehicle is another critical requirement for the mission analysis and architecture assessment. Indeed, while the Ariane 64 version will be able to inject heavy payloads into Earth escape orbits, this launcher is still under development and there are currently some uncertainties on its performance and potential limitations for interplanetary missions. These include the available number of flight programs, admissible values of the Declination of the Launch Asymptote (DLA), and penalty associated with high declination escapes. These parameters have a direct impact on the spacecraft Delta-V sizing and so conservative assumptions had to be taken, resulting in a launch mass minimisation challenge, in addition to the aforementioned timeline constraints.

3. INTERPLANETARY TRANSFERS

The selection of the outbound (Earth-Mars) and inbound (Mars-Earth) interplanetary transfers are the primary drivers for both the overall mission timeline (dates and durations) as well as the spacecraft sizing (propellant load). As described in the previous section, the ERO mission is characterised by challenging timeline and mass requirements. The mission analysis for the interplanetary transfers therefore has to consider two common but antagonistic optimisation objectives, namely aiming at minimising the transfer duration and required Delta-V. In order to offer a variety of system design options for the architecture assessment, interplanetary

transfers with both Chemical Propulsion (CP) and Electric Propulsion (EP) have been optimised, respectively described in the next paragraphs.

3.1. Interplanetary Transfers With Chemical Propulsion

Energy optimal opportunities for ballistic Earth to Mars and Mars to Earth transfers are well known and documented for the years considered for the mission. Key parameters for the evaluation of the architectures are the hyperbolic excess velocity (V-infinity) for departure (launcher performance) and arrival (Mars Orbit Insertion), together with the departure and arrival dates (timeline). These are illustrated by the opportunity maps on Figure 2 below, for short (direct) transfers between 2026 and 2030. Another parameter of importance is the declination of the asymptote of the hyperbolic orbit (δ, angle to the equator), both for the Earth escape (possible launcher restrictions), Mars arrival and departure (compatibility with inclination of the orbit at Mars, see dedicated section).

Transfers using Deep Space Manoeuvres (DSM) and/or Earth Gravity Assists (EGA) have also been considered, in particular for cases constrained by a zero declination launch (higher injection mass for a given escape C3 with the considered launcher performance model), as well as slightly suboptimal transfers in order to allow flexibility in the transfer dates (typically to increase the duration at Mars i.e. to advance the Mars arrival or delay the Mars departure) at the expense of an increased Delta-V and therefore mass penalty. Figure 3 illustrates sample CP transfer trajectories both, for the outbound (direct 2026-T2 CP transfer, left figure) and the inbound legs (direct 2028-T2 CP transfer with two weeks Mars delayed departure, right figure).

3.2. Interplanetary Transfers With Solar Electric Propulsion (SEP)

The use of Solar Electric Propulsion for the interplanetary transfers can serve different purposes, depending on the phase of the mission. For the outbound transfer, EP is a useful way to reduce the Earth departure V-infinity and therefore increase the available launch mass, also enabling to perform the launch declination corrections that may be required with a lesser propellant mass impact as compared to CP. It also provides the opportunity for a significant reduction of the Mars arrival V-infinity, thus decreasing the required Mars Orbit Insertion (MOI, discussed in another section of the paper) Delta-V, which always requires the high thrust offered by CP unless the approach velocity is reduced down to 0 (ballistic capture). In a similar way, for the return transfer, EP can be used to lower the Mars departure V-infinity, reducing the magnitude of the Trans-Earth Injection (TEI) Delta-V, and/or to lower the Earth arrival V-infinity to reduce aerothermodynamic loads on the ERC during the atmospheric arc. In most cases however, this has been found to be not necessary given the requirements on the Earth entry velocity, as an Earth arrival

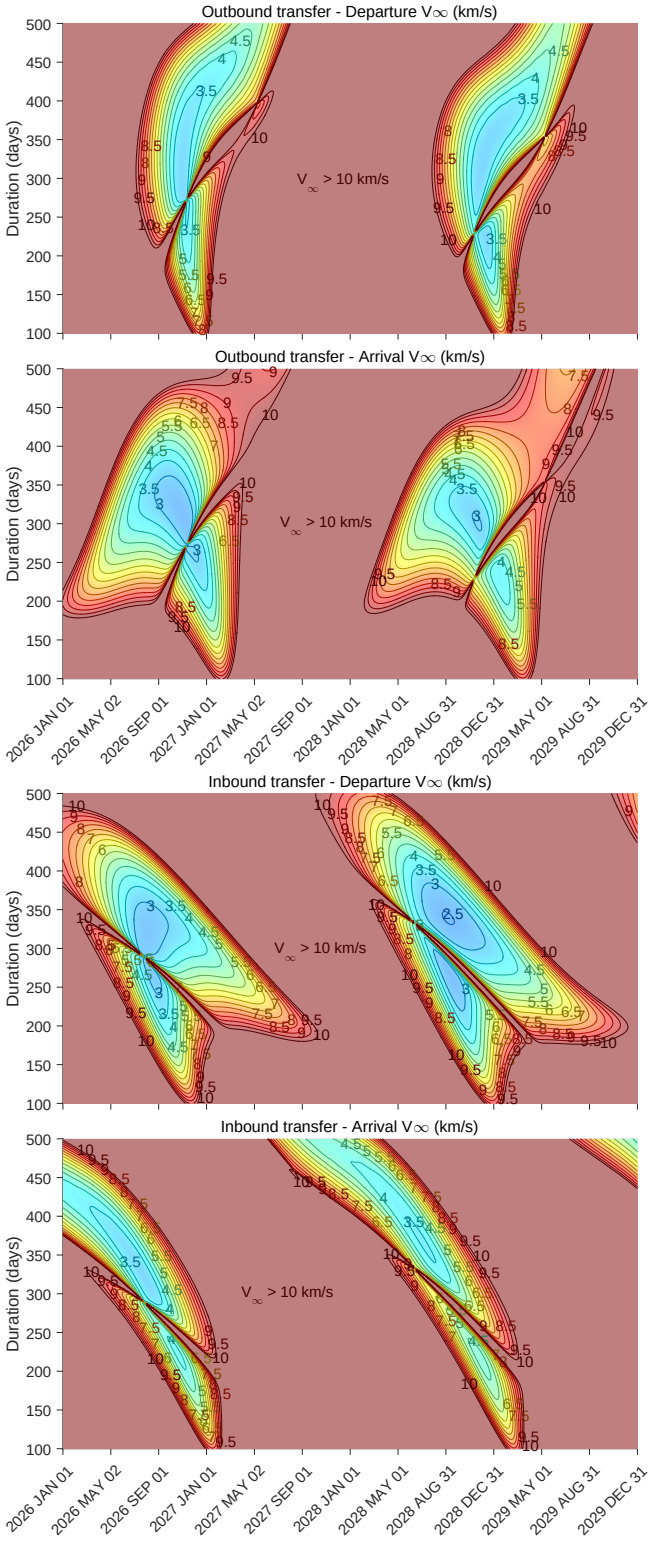

Fig. 2. 2026-2030 ballistic outbound and inbound transfers opportunity maps (*porkchop* plots)

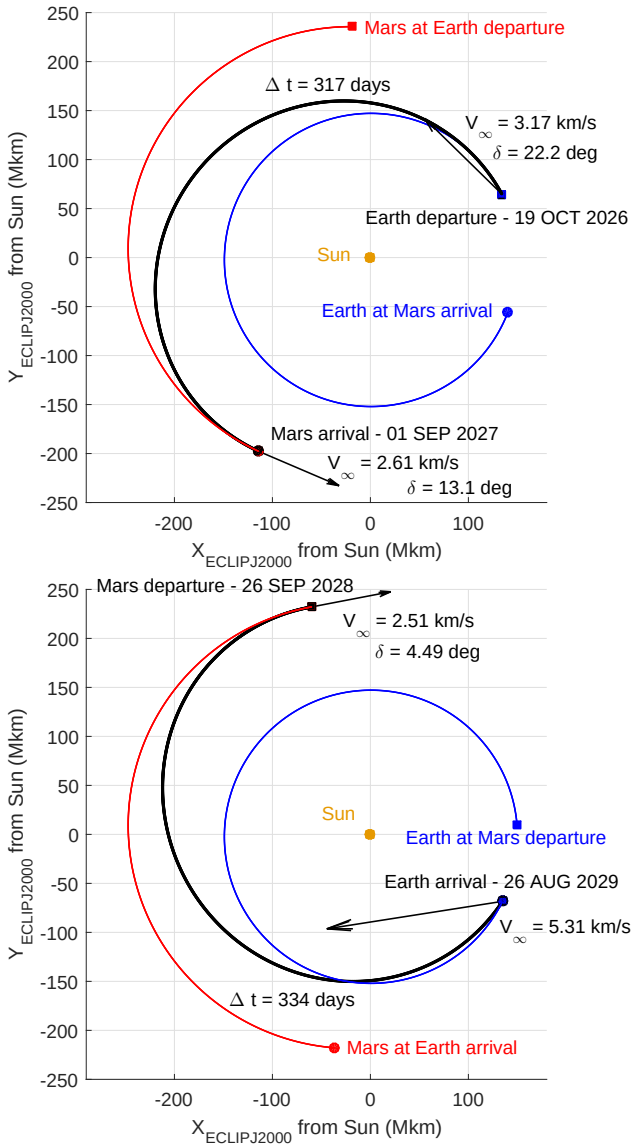

Fig. 3. Sample outbound (top, 2026-T2) and inbound (bottom, 2028-T2) CP transfers

V-infinity of up to about 6.8 km/s is considered acceptable. In both outbound and inbound cases, an important point is that SEP also brings additional freedom in the timeline definition, as the Delta-V penalty incurred by deviating from the energy optimal transfer (departure and arrival) dates is much lower than for CP transfers.

On the other hand, the design of interplanetary missions with SEP is made more complex by the very strong interactions that exist between the spacecraft design and the transfer properties. In particular, a key driving parameter for the trajectory design is the available power for the Electric Propulsion System (EPS), generally defined by the value at 1 au and the model for its evolution with the heliocentric distance. While the maximum available power from the Sun follows an inverse squared law, the size (and technology) of the Solar Arrays, the number and type of thrusters, as well as the possibility to throttle the engines to change the operating points as the EPS input power varies, are all parameters that drive the thrust to mass ratio (and the Isp) along the transfer. Finally, SEP interplanetary transfers are also more complex operationally than classical CP transfers: the concept of navigation and the associated performance of Orbit Determination (OD) have not been analysed in the context of the present study, but low-thrust transfer operations are likely to require some forced coast arcs for navigation and orbit correction, in particular prior to critical events such as planetary insertion.

Figure 4 illustrates two sample outbound EP transfers. The first (left figure) has been optimised using a constant thrust model, meaning that the power is sized to ensure the EPS is fully powered at Mars. In this example, departure and arrival dates are not too far from the classical CP solutions, but the use of EP enables a reduction of the Earth escape V-infinity (typically around 3 km/s for CP optimal transfers and reduced to about 2.23 km/s on this example), a near equatorial launch, as well as a large reduction of the Mars arrival V-infinity, down to about 1.47 km/s. This comes at the expense of a significant SEP Delta-V (2.59 km/s), however the high Isp (3900 s on this example) of the propulsion system results overall in an increased mass efficiency, measured in mass delivered at Mars.[1] The second example (right figure) corresponds to a higher power case for which the spacecraft departs Earth much earlier, far from the classical ballistic transfer solution. In this example, the Earth escape velocity is further reduced down to about 2.08 km/s, and essentially EP provides the conditions for a ballistic capture at Mars, bringing the Mars arrival velocity down to 0 and therefore removing the need for an expensive chemical MOI. This solution is characterised by an intermediary coast arc between two thrust arcs whose total Delta-V amounts to 5.94 km/s.

A large number of SEP transfers have been optimised during the MSR architecture study, with a parametric variation on the departure and arrival dates, departure and arrival V-infinity (considering both equatorial constrained and free launch declination), thrust-to-mass ratios (at 1 au), and simplified thrust evolution model with heliocentric distance (constant thrust, inverse and inverse squared). This parametric analysis has resulted in a large transfers database (above a thousand SEP transfer solutions) in which the best fit for a given mission and spacecraft architecture can be selected.

[1] With the considered Launch Vehicle performance model, the maximum mass delivered at Mars in the High Elliptical Orbit post-MOI is of about 3750 kg for the previously shown 2026 short CP transfer, compared to nearly 5150 kg for the EP (hybrid) first transfer illustrated on Figure 4.

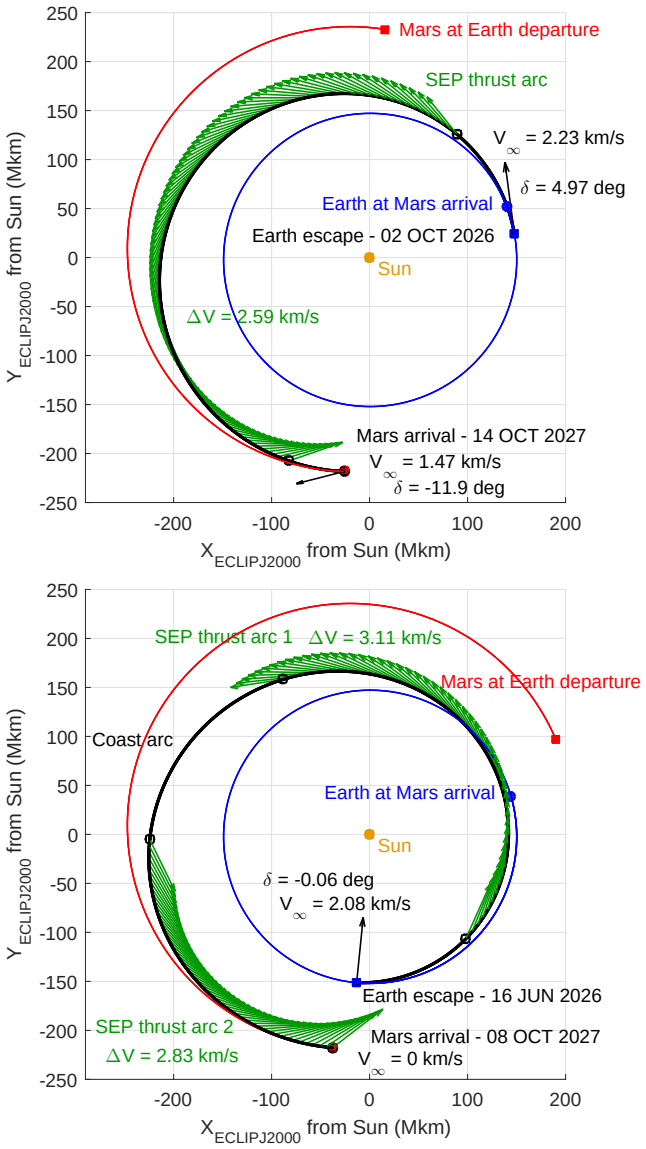

Fig. 4. Sample outbound SEP transfers: the thrust arcs represented by the green arrows

4. LOW MARS ORBIT INCLINATION TRADE-OFF

This section summarises the trade-off performed regarding the inclination of the orbit at Mars, as this parameter has direct consequences on the operations at Mars, presented in the next section.

The initial requirements for the Low Mars Orbit (LMO) were based on mission concepts involving a NASA led orbiter (Next Mars Orbiter, NeMO), whose mission included scientific objectives calling for a high inclination, around 70 to 75 deg, in order to ensure coverage of the polar regions. In the case of an ESA-led Earth Return Orbiter (ERO) mission concept however, the LMO inclination is no longer driven by science considerations and it was agreed with the Agency to re-open the LMO inclination trade-off early during the study. The primary driver for the selection of the LMO is to ensure compatibility with the launch site as well as with the reachable orbit and associated performance of the Mars Ascent Vehicle (MAV) injecting the Orbiting Sample (OS) in orbit around Mars. With the objective to assess the opportunity offered by this additional degree of freedom to improve the mission architecture, the next paragraphs describe the main criteria considered for the LMO inclination trade-off and conclude by the proposed baseline for an updated LMO inclination.

4.1. Absolute RAAN Drift Considerations

At a similar altitude, the J_2 perturbation on a Low Mars Orbit is stronger than on a Low Earth Orbit. It causes a secular drift rate of the Right Ascension of the Ascending Node (RAAN), as well as the Argument of Pericentre (AoP), in the case of an elliptical orbit. In LMO, the RAAN drift rate varies significantly with the (circular orbit) altitude and inclination. The left contour map on Figure 5 shows the variation of the RAAN drift rate (iso-lines) for a range of inclinations (X-axis) and altitudes (Y-axis) in LMO, based on the first order analytical expression of the secular RAAN drift rate expression. The figure on the right converts this drift rate in number of days required for the line of nodes to complete a 180 deg rotation.

As can be seen on the previous plots, for a given altitude, the inclination has a strong impact on the absolute RAAN drift rate, especially at low altitudes: the lower the inclination, the faster the RAAN drift. For example the RAAN drift rate at 343 km is of about -3 deg / day on a 75 deg inclined orbit and reaches about -10 deg / day for a 25 deg inclination. This has a direct consequence on the time needed to reach the necessary conditions for the interplanetary escape (Departure Orbit Acquisition). Indeed, for a given date and Mars escape conditions (V-infinity vector), two values of the RAAN are generally admissible.[2] As an out-of-plane manoeuvre to actively modify the RAAN would come at a prohibitive Delta-V cost, the strategy relies on using this natural drift as a passive way, thus favouring low inclinations to limit the time required to reach the departure RAAN.

4.2. Relative RAAN Drift Between the ERO and the OS After MAV Launch

The LMO inclination also drives the *relative* RAAN phasing duration between the ERO and the OS once injected into Mars orbit, as a consequence of the same physical phenomenon (secular drift of the line of nodes caused by the planet's oblateness). The MAV injection dispersions (typical 3σ injection errors $\Delta a = \pm 30$ km, $\Delta e \leq 0.02$, $\Delta i = \pm 0.5$ deg) together with the performance of the Orbit Determination for

[2] only one if the inclination is equal to the departure declination, and none if the inclination is lower (no solution).

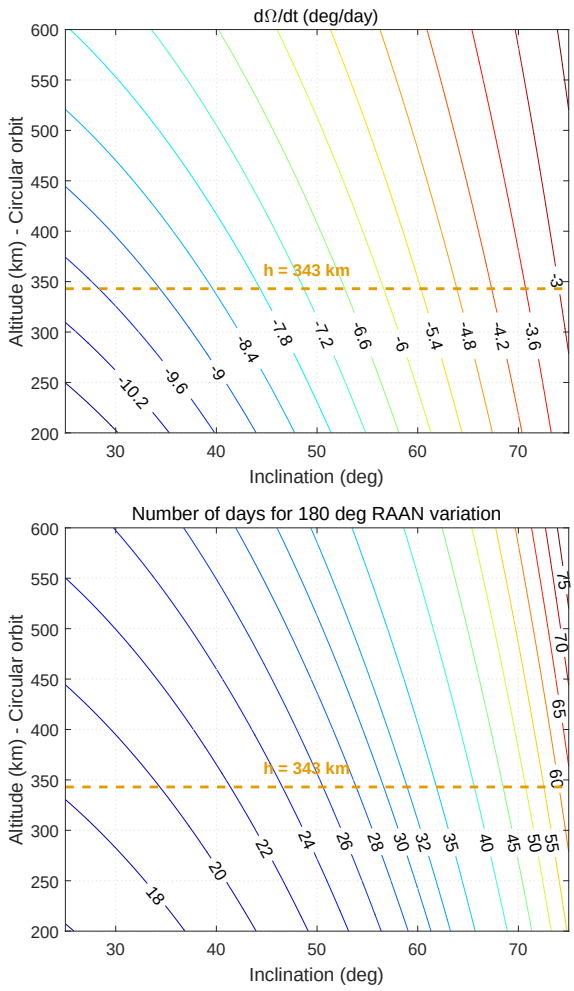

Fig. 5. Absolute RAAN (Ω) drift rate (left) and duration for 180 deg drift (right)

the orbiter lead to consider a minimum altitude differential between the orbiter and the OS prior to rendezvous. The OS must therefore be launched with also a RAAN differential with respect to the orbiter, such that the difference in RAAN drift rate passively allows the orbital planes to match during the time allocated for the rendezvous operations.[3]

In the initial MSRO study, the MAV launch was required to occur close to noon Local Solar Time (LST), which, at a given epoch, constrains the admissible RAAN for the OS at injection. Rigorously, two situations must be distinguished: either the target inclination is equal to the latitude of the launch pad (calling for a launch towards East with an azimuth of 90 deg), in which case the launch local time constraint imposes a single RAAN value for the OS injection, or the inclination is strictly greater than the latitude of the launch pad, in which case there are two possible values for the RAAN (corresponding to a launch towards North or towards South). This is illustrated by the Figure 6 below on which a given orbital inclination is reached from different launch sites: two RAAN values are admissible only if the latitude of the launch site is lower than the target inclination.

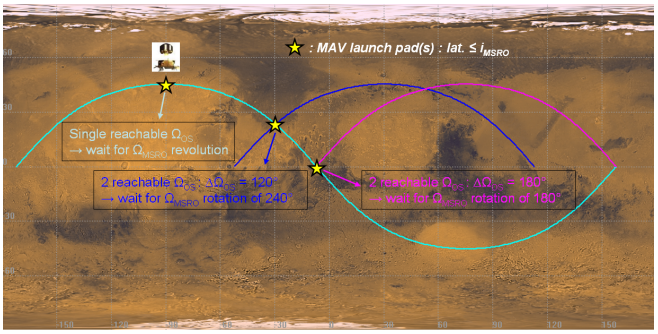

Fig. 6. Reachable RAAN for different MAV latitude (illustration purpose)

In any case, a constraint on the MAV launch solar time could possibly lead to long relative RAAN phasing durations. However, the current baseline for the MAV is that the requirement on a fixed local solar time for the launch is no longer applicable. It is therefore assumed that the OS is launched directly in a plane close to that of the orbiter, the initial RAAN differential being only driven by their altitude differential. In those conditions, a slower relative drift rate (and therefore higher inclination) is preferable, as it enables a smaller initial plane separation for a given altitude differential, thus facilitating the OS detection.

4.3. Earth Visibility During MAV Ascent

Another aspect related to the MAV launch is that the ERO is required to be in visibility of Earth during the ascent. As already discussed in the previous paragraph, a given LMO orbit can generally be reached by the MAV twice a day, as long as the inclination is greater than the launch pad latitude. For a given launch pad latitude, higher inclinations lead to a larger longitude or Right Ascension (RA) separation of the two launch opportunities. For example, in the case of an equatorial launch, the two opportunities (ascending and descending nodes) are always separated by a maximum value of 180 deg for all (non-zero) target inclinations. This is illustrated by Figure 7 below: the left contour map shows the RA separation of the two launch opportunities (when applicable) as a function of the inclination (X-axis) and for various latitudes of the launch pad (one curve per latitude).

A larger separation in the Right Ascension of the launch opportunities increases the chances of having good visibility

[3]The initial RAAN separation, driven by the inertial longitude (or local time) of the MAV launch, must be large enough to ensure there is no RAAN overshoot during that time. On the other hand, the initial plane separation cannot be too large, otherwise the orbiter would not be able to perform the OS detection right after the MAV injection. Here again, for a given altitude differential, a lower inclination leads to a faster relative RAAN drift.

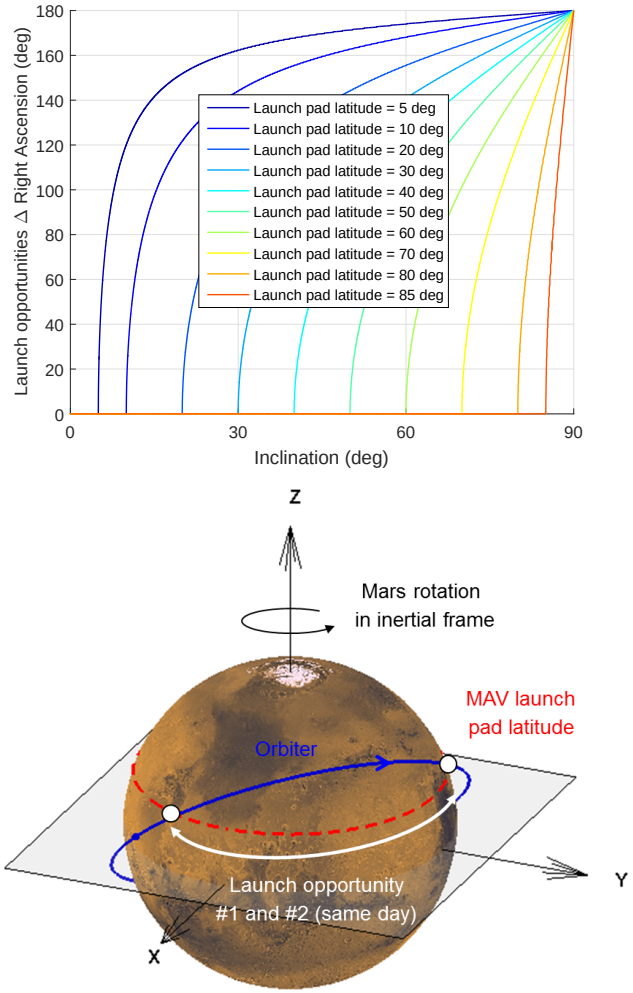

Fig. 7. Launch opportunities RA separation as a function of inclination and launch pad latitude (left), illustration with $i = 40$ deg and latitude = 20 deg (right)

conditions for Earth communications for at least one of the two. From this perspective, higher inclinations are therefore more favourable.

4.4. Impact of the LMO Inclination on Eclipses Conditions

Finally, the inclination of the LMO has an impact on the lighting conditions in orbit, as well as on the duration of the eclipses at Mars. For a circular orbit, the duration of the eclipses are driven by the value of the solar β angle, defined as the angle between the orbital plane and the Sun vector. The instantaneous value of the solar β angle is a function of the orbit's inclination, RAAN, and of the areocentric solar longitude Ls (period within the year, Mars season). It is however always bounded by $\pm\beta_{\max} = i + \epsilon$, where i is the inclination of the orbit and ϵ is the angle between Mars' equatorial plane and the ecliptic, around 25.19 deg. The next Figure 8 illustrates the duration of the eclipses per orbit[4] around Mars as a function of the solar β angle on the baseline 343 km ($\pm$30 km) altitude orbit, as well as the maximum value this parameter can reach ($\beta_{\max}$, orange dashed lines) for various inclinations between 0 and 40 deg.

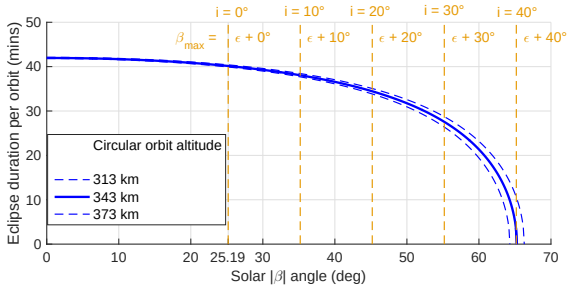

Fig. 8. Eclipses duration as a function of the solar β angle

It has to be noted that, whatever the inclination, the solar β angle can always take the value of 0 (Sun in the orbital plane), which corresponds to the worst-case (longest) eclipse durations, around 42 minutes. However, the *minimum* eclipse duration (for $\beta = \beta_{\max}$) is indeed a function of the inclination: the higher the inclination the lower the minimum eclipse duration (e.g. down to 0 for 40 deg inclination). On the other hand, there will be eclipses every orbit for $i \leq 40$ deg and if the inclination is very low (e.g. below 20 deg), then eclipses will always be long (e.g. more than about 35 minutes), regardless of the RAAN and season.

4.5. LMO Inclination Trade-Off Summary and Proposed Baseline

Table 1 provides a summary of the inclination trade-off:

Table 1. LMO inclination trade-off summary

Trade-off criteria	Preferred inclination: rationale
RAAN absolute drift	Low: Faster phasing for DOA
RAAN relative drift	High: OS detection, Orbit Matching
MAV launch ΔRA	High: Earth comms during ascent
Eclipses min duration	High: Power, thermal, rendezvous
MAV compatibility	min: launch pad lat. max: performance limitation
Transfers compatibility	min: |declination|

A preliminary baseline of about 40 deg has been proposed and agreed by ESA and JPL for further analysis. This value was found to be a good compromise between the identified trade-off criteria, compatible with all candidate launch sites for the MAV and always higher than Mars arrival and departure declination (compatible with interplanetary transfers).

[4]The orbital period for a circular orbit at 343 km is about 1 hour 56 minutes.

5. MARS OPERATIONS

5.1. Mars Arrival and Mars Orbit Insertion (MOI)

Upon completion of the outbound transfer, the Mars Orbit Insertion is achieved by performing a large retrograde manoeuvre around the pericentre of the hyperbolic approach orbit. For a given transfer and therefore Mars arrival conditions (V-infinity magnitude, declination δ, and Right Ascension RA), there is set of possible triplets (inclination i, Argument of Pericentre ω, RAAN Ω) matching the arrival hyperbolic trajectory. The selection of the actual orbit can be achieved at a limited Delta-V cost by B-plane targeting prior to Mars arrival. Figure 9 and Figure 10 illustrate these reachable orbits for a sample 2026 fast outbound transfer (arrival on 24 September 2027, Vinf = 2.57 km/s, RA = 115 deg, δ = -16.7 deg with respect to the Mars equatorial plane), assuming a pericentre altitude of 300 km: both prograde and retrograde orbits are shown. Each colour represents a given value of the B-angle. The bottom-left figure illustrates the geometry of a sample subset: both the hyperbolic orbit prior to MOI and the reached High Elliptical Orbit (HEO) are shown.

As can be seen from the figure, the minimum inclination is equal to the (absolute value of the) arrival declination δ, and there is a symmetry between prograde ($i < 90$ deg) and retrograde ($i > 90$ deg) orbits with respect to the polar inclination ($i = 90$ deg) for the reachable values of argument of pericentre. However, if the inclination is fixed and strictly within the interval $[|\delta|, \pi - |\delta|]$, two orbits are then compatible with the arrival hyperbola. The bottom-right figure on Figure 9 shows two such insertions, corresponding to the same inclination of 40 deg, also identified by the dashed lines on the two top figures. These are characterised by different values of the RAAN, slightly different values of the local solar time at insertion, but essentially different values of the argument of pericentre, driving in particular the latitude of the apocentre of the HEO. This is likely to be the main driver to select between the two, based on the most favourable geometry for communications with Earth, communications between the orbiter and the lander (see next section), as well as lighting and eclipses conditions (for example avoiding placing the apocentre in eclipse).

Another critical aspect linked to the MOI is the assessment of the *gravity losses* associated with the finite thrust burn. A standard assumption of a 4-sol HEO orbit post-MOI, corresponding to an apocentre altitude of about 96000 km, has been considered during the study. Owing to the large Delta-V required to reach this orbit, a high-thrust chemical propulsion system (1100 N thrust) has been considered to limit the Delta-V penalty. Gravity losses have been systematically computed for all candidate interplanetary transfers (Mars arrival V-infinity), and thrust-to-mass ratios.

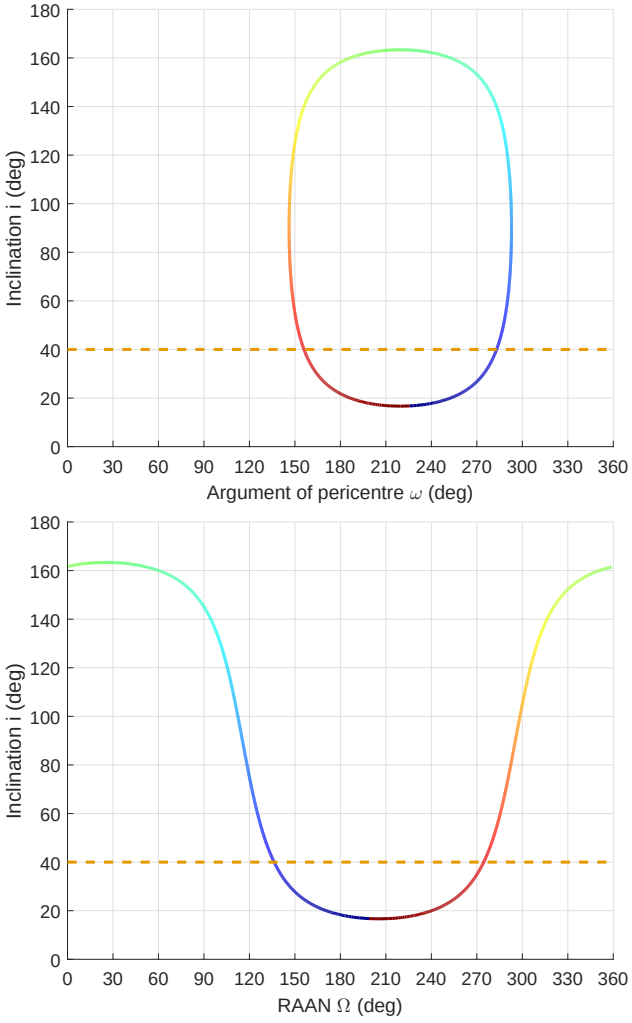

Fig. 9. MOI reachable orbits (i,ω,Ω) for a sample interplanetary transfer

5.2. Target Orbit Acquisition (TOA): Chemical Apocentre Reduction and Aerobraking (A/B)

After MOI, a chemical apocentre reduction is initiated before the aerobraking (A/B) begins, if applicable. A preliminary baseline, corresponding to the A/B scenario for the ExoMars Trace Gas Orbiter (TGO), is to start A/B with an apocentre at an altitude corresponding to a 1-sol orbital period. Assuming that the post-MOI HEO orbit is a 4-sol orbit, the spacecraft needs to perform a manoeuvre ($\Delta V = 137$ m/s) to lower the apocentre from 96000 km to about 34000 km. However, this initial A/B apocentre altitude can be optimized to better fit the needs of the mission architecture and timeline: Figure 11 below shows the Delta-V from MOI to the initial A/B orbit (Y-axis, left) and corresponding orbital period (Y-axis, right) as a function of initial A/B apocentre altitude (X-axis).

The motivations to modify the initial A/B apocentre altitude can be either to:

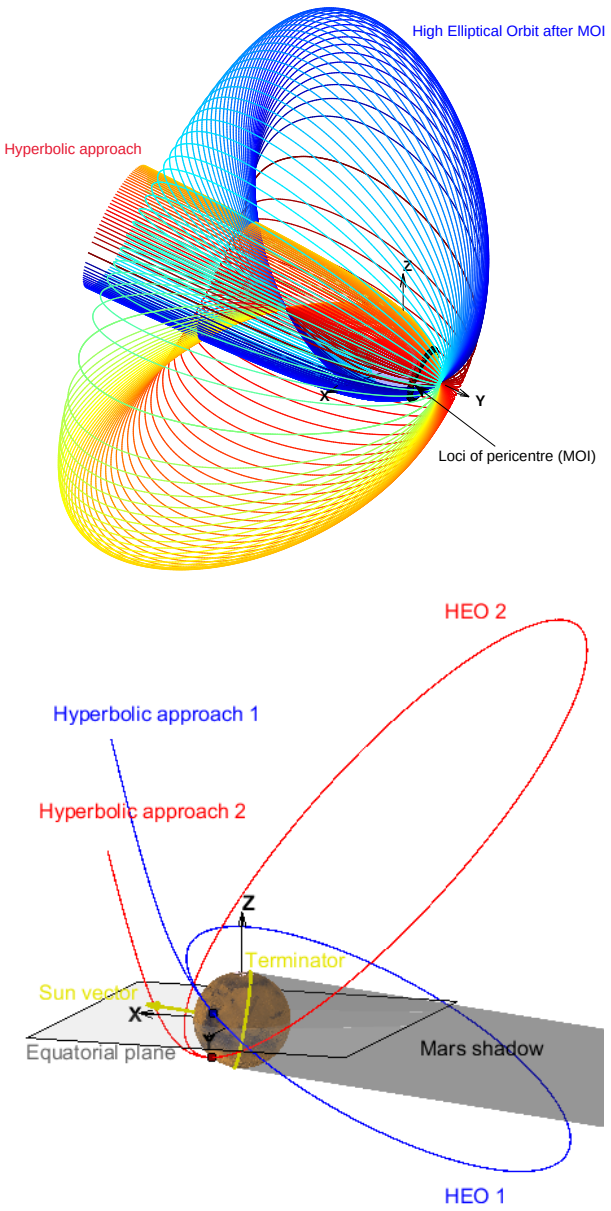

Fig. 10. MOI geometry and cases for $i = 40$ deg

- decrease the chemical apocentre reduction Delta-V, by starting A/B from a higher apocentre: the maximum Delta-V saving is of 137 m/s. This however increases the A/B duration.

- decrease the A/B duration, by starting the A/B from a lower apocentre: however the Delta-V increases rapidly as the initial apocentre decreases (left blue curve on the figure). To the limit, no A/B is performed and the TOA is entirely performed by a sequence of CP apocentre reduction manoeuvres, in which case the total Delta-V amounts to about 1323 m/s.

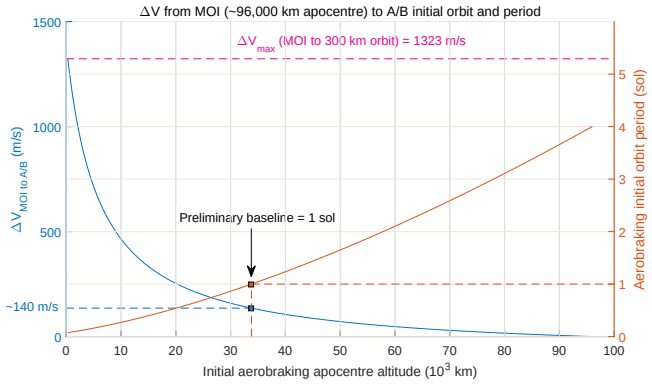

Fig. 11. Initial aerobraking apocentre altitude trade-off

To initiate A/B, the pericentre of the orbit is progressively lowered (*walk-in*) into the Martian atmosphere, carefully monitoring the loads imposed on the spacecraft, until the target dynamic pressure peak value (key sizing parameter for the spacecraft design, together with the heat flux) is reached. A pericentre altitude between 110 km and 120 km is typically considered for A/B at Mars. Only small manoeuvres are then needed to control the pericentre altitude and maintain the dynamic pressure peak in order to maximise the efficiency of the apocentre lowering without compromising the integrity of the spacecraft. At the end of A/B, a *walk-out* sequence gradually raises the pericentre out of the atmosphere, which is the most Delta-V consuming phase (circa 90 m/s).

A detailed simulation and optimisation of the A/B scenario for all investigated architectures is outside the scope of the study, and the architecture assessment has been based on heritage studies as well as inputs provided by ESA in the form of a parametric analysis of the impact of the ballistic coefficient ($B = \frac{m}{AC_D}$, where m is the mass of the spacecraft, A the cross-sectional area, and C_D the drag coefficient), and peak dynamic pressure (P_{dyn}, typically between 0.3 N/m^2 and 0.5 N/m^2). Both these parameters have a critical impact, both on the spacecraft design and on the mission timeline. For architectures with a particularly tight timeline, a harsh A/B with high dynamic pressure peak (0.5 N/m^2) and low ballistic coefficient (down to about 40 kg/m^2) has been baselined.

5.3. Communications With Lander During Aerobraking

In this section, an overview of the analysis of the landing site visibility conditions from the ERO during A/B is presented. The objective of this analysis is to assess the possibility to communicate with a terminal on the Martian surface (Sample Return Lander, SRL) while aerobraking. Two landing sites have been considered during the study: Jezero Crater (latitude = 18.44 deg, longitude = 77.50 deg), and Columbia Hills (latitude = -14.55 deg, longitude = 175.63 deg).

Several parameters come into play for a detailed analysis of such scenarios, starting by the evolution of the geometry of

the orbit with respect to the Martian surface. As previously discussed, the detailed optimisation and end-to-end simulation of the aerobraking trajectory was beyond the scope of the study, so a simple approach has been followed: the apocentre altitude profile is assumed to be decreasing linearly with time throughout the whole A/B sequence, the pericentre is assumed to be maintained at a constant altitude of 120 km[5], the evolutions of the RAAN and AoP are driven by the first-order secular drift rate due to Mars J_2 only (both these drift rates change throughout A/B as the semi-major axis and eccentricity gradually decrease), and finally the inclination is assumed to remain constant (40 deg). These assumptions led to consider a semi-analytical orbit propagation model, where only 3 orbital parameters are propagated, namely the true anomaly, RAAN and AoP. This model only approximates the complex dynamics involved during A/B: no other Gravity Harmonics than J_2, no solar perturbation, and the drag effect and pericentre correction manoeuvres are not simulated, as the evolution of apocentre and pericentre altitudes are assumed a priori. A ballistic coefficient of 50 kg/m^2 and a peak dynamic pressure of 0.5 N/m^2 are assumed, resulting in an A/B duration of 205 days. Figure 12 below represents the corresponding evolution of the orbit during A/B: the two first figures illustrate 30 sample orbits (each separated by about one week), with the dots on the middle figure showing the position of the osculating pericentre. The latitude of Jezero crater is shown in white dashed line. The right figure shows the evolution of the RAAN (decreasing) and AoP (increasing), with the dots representing the sample orbits on the first two figures.

As evidenced by the figures, the combined effect of RAAN and AoP drift due to Mars' J_2 and apocentre reduction results in a complex orbit evolution over the A/B duration. The position of the pericentre varies both in latitude (remaining bounded by $\pm i$) due to the variation of the AoP, and in (inertial) longitude, due to the RAAN drift. The change rate of the orbit is increased near the end of A/B, where the semi-major axis is minimal and both RAAN and AoP drift rates are faster.

Once these orbits are propagated in an inertial frame, the remaining degree of freedom for the communications analysis is the (initial) Martian longitude of the pericentre, defined with respect to the (non-inertial) Martian surface. As was described in the previous paragraphs, the initial Right Ascension of the Ascending Node (RAAN) and Argument of Pericentre (AoP) with respect to a Mars-centred inertial frame are defined by the Mars arrival conditions after MOI. However the actual Martian *longitude* (with respect to a Mars Body-Centred Body Fixed frame, rotating with respect to the inertial frame) of a given reference point on the orbit (typically the pericentre) can be tuned to any value by proper arrival timing, with only minor implications on the transfer Delta-V.

A parametric analysis was conducted to assess the impact

[5]In particular, it is assumed for this analysis that there is no interruption of the aerobraking (walk-out, due to solar conjunction event for example).

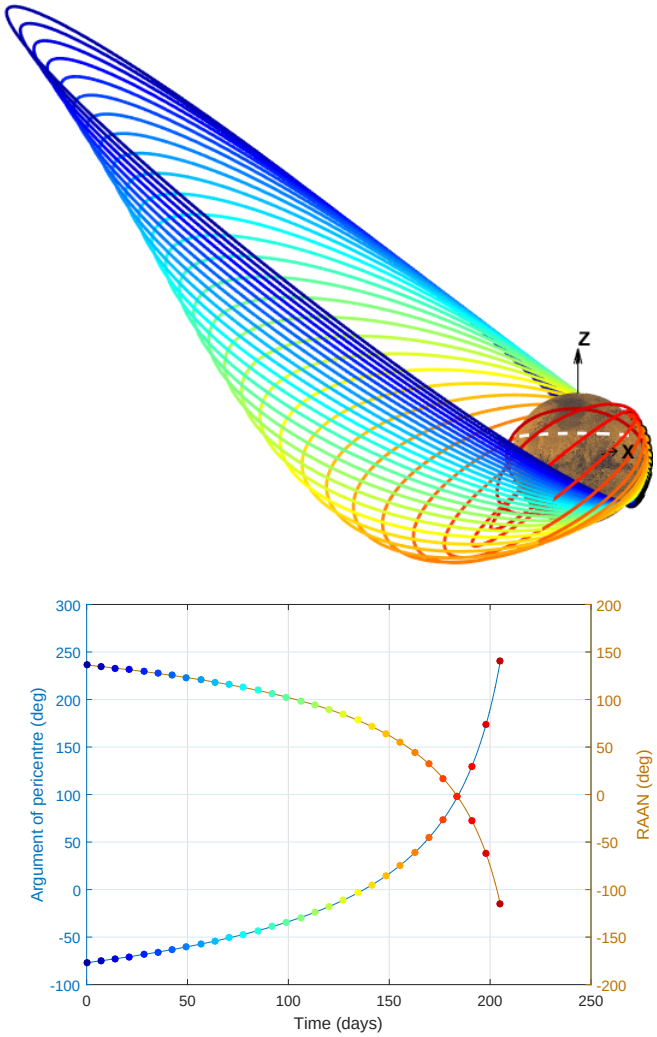

Fig. 12. Aerobraking orbit semi-analytical propagation results (30 sample orbits)

of the initial pericentre longitude on the contact times with the lander, for both landing sites, for the two reachable orbits (2 admissible values of AoP) corresponding to a sample interplanetary transfer (the same as in the previous paragraph), and in two situations: either communications between the ERO and the SRL can occur at any time of day, or they are only possible during daytime (positive Sun elevation as seen from the SRL on the Martian surface). Figure 13 shows the cumulated contact duration between the ERO (single AoP case) and a lander located at Jezero as a function of time, assuming a *minimum elevation angle* of 10 deg, a *minimum altitude* of 350 km (under this altitude, A/B operations take priority) and a *maximum range* of 20000 km. Each curve corresponds to a given assumption for the initial longitude of the pericentre: longitudes between 0 and 360 deg (step of 1 deg) have been simulated.

It can be seen that the overall profile of the cumulated

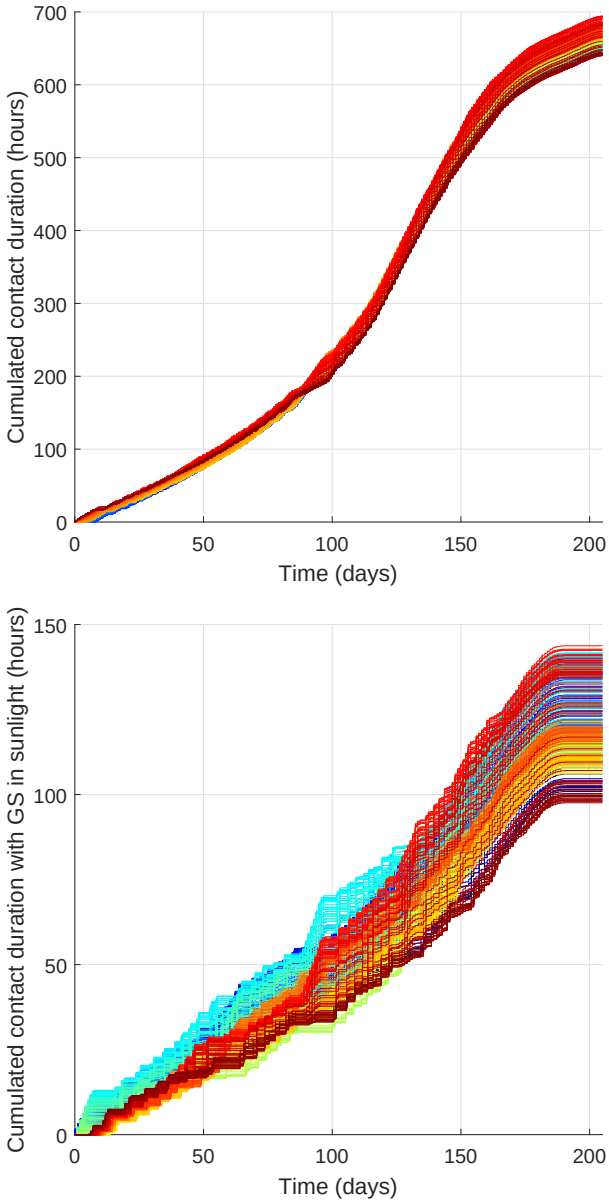

Fig. 13. Cumulated contact duration with Jezero Crater Ground Station (GS) as a function of time during A/B, without (left), and with (right) daytime constraint: each curve represents a given assumption for the initial longitude of the pericentre

contact duration is not impacted too much by the initial value of the pericentre longitude, with less than 10% difference between the final minimum and maximum. However, the selection of a given initial longitude can lead to significant differences on a specific day, especially when the daytime constraint is taken into account. Figure 14 represents in a bar chart (left) the contact time for each day, with (red) or without (blue) the daytime constraint, as well as the local solar time of each visibility slot (right). This analysis is carried out for a single value of the pericentre longitude, selected such that the cumulated contact duration with the SRL is maximised, while also ensuring good conditions during the first day of A/B. On this example, most communication slots occur at when the Sun is below the (SRL) horizon, which explains the observed difference in cumulated contact time with and without the daytime constraint.

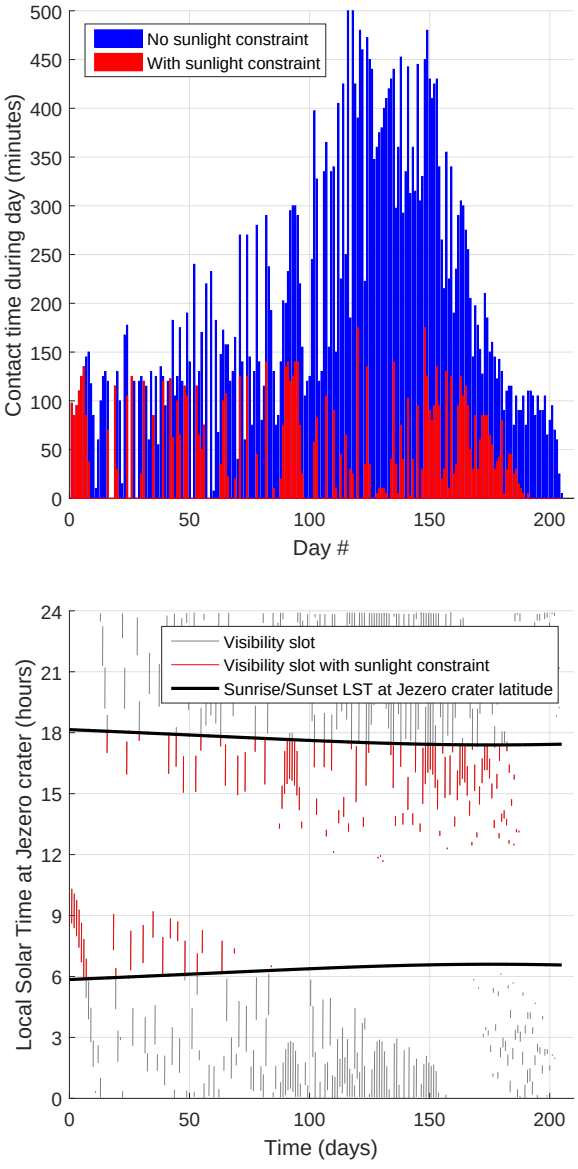

Fig. 14. Orbiter-lander contact duration per day and local solar time of contacts

5.4. Rendezvous and Mars Operations Until Trans-Earth Injection (TEI)

Table 2 below presents the main phases occurring after the ERO reaches the operational LMO, between MAV ascent until Trans-Earth Injection (TEI).A preliminary timeline is proposed based on the updated LMO inclination, and assuming that CP is used for all manoeuvres, including rendezvous and apocentre raising after the OS capture.

The rendezvous strategy was investigated in detail during the previous MSRO Phase A. For that study, the baseline altitude for the OS was significantly higher (500 km) than the present assumption (343 km), so the detailed scenario would need to be updated, but the principles remain the same.

In the absence of a MAV launch time constraint, the OS is injected into a near-circular orbit lower than the orbiter, at the same inclination and with a RAAN close to the RAAN of the ERO, with just enough separation to allow for a passive plane matching caused by the altitude differential, during the time required for the rendezvous operations. The OS detection phase starts directly after the MAV ascent and OS release, using both an RF sensor and a Narrow Angle Camera (NAC). The Orbit Determination (OD) of the OS is performed using these relative measurements together with absolute navigation and ground-processing for an accurate restitution of the orbit. Owing to the relatively far range of the RF sensor, RF detection slots generally last a few hours, while the NAC optical detection slots typically last tens of minutes, and are separated by tens of hours up to a few days depending on the exact altitude differential. After OS detection, a relatively large *Homing*-like couple of manoeuvres (Hohmann transfer) is performed by the ERO to cancel most of the altitude differential, bringing the orbiter within a closer distance to the OS (about 120 km along-track). The nominal manoeuvre, performed in open-loop, is such that it does not cancel the entire altitude differential in order to avoid collision risks resulting from errors in the realisation of the boosts.

The subsequent approach is then typically performed by means of a succession of smaller manoeuvres, progressively decreasing the altitude differential as well as the along-track distance (true anomaly differential) in a so-called *co-elliptic* approach. During this phase, a closer range sensor (e.g. Wide Angle Camera) and eventually a LiDAR are acquired, at distances of about 50 km and 5 km respectively. These are then used for the very final approach (from about 100 m), performed in closed-loop along a forced translation trajectory, until capture and bio-sealing of the samples.

After the OS capture, the orbiter finally needs to reach the RAAN required for the Trans-Earth injection (TEI) initiating the return interplanetary transfer. With the lower baseline inclination (40 deg), it is assumed for the timeline estimate that the absolute RAAN drift could cover 200 deg, therefore requiring up to about 24 days. The apocentre of the orbit is then raised again through a succession of (CP) manoeuvres before TEI is performed. Electric Orbit Raising (EOR) strategies have also been investigated for some hybrid mission architectures.

6. EARTH RE-ENTRY CONDITIONS

In a similar way that the Mars arrival conditions after the outbound interplanetary transfer drive the possible orbits at Mars, the Earth arrival conditions after the return transfer drive the admissible re-entry trajectories. Figure 15 below illustrates such trajectories after a sample CP transfer:

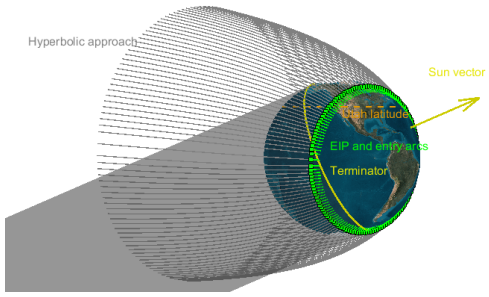

Fig. 15. Hyperbolic approach and admissible Earth re-entry trajectories for a sample inbound transfer (CP 2028-T1 Mars-Earth) and FPA=-11 deg at EIP

The entry trajectory characteristics are influenced by the initial entry relative (atmospheric) velocity[6] and the Flight Path Angle (FPA, angle of the velocity vector to the local horizontal plane) at the Entry Interface Point (EIP), typically defined by a geocentric altitude of 120 km. These parameters determine the aerothermodynamic loads during the atmospheric arc and therefore represent strong drivers for the design of the Earth Re-entry Capsule (ERC). The FPA angle can be chosen freely without Delta-V penalty via approach orbit pericentre altitude targeting: entry angles between -8 deg (shallow) and -15 deg (steep) are often considered. This angle, together with the aerodynamic properties of the vehicle, determines the subsequent entry arc length from EIP to impact.

The assessment of the candidate mission architectures and associated selection of interplanetary transfers must therefore be done including the systematic verification of the compatibility with Earth re-entry requirements, such as target landing site and potential constraints about local solar time (e.g. night re-entry). Figure 16 below shows the analyses conducted to verify compliance with such requirements for the arrival conditions illustrated on the above figure: the left plot represents for various values of the FPA (colours) the admissible EIP

[6]The relative velocity is driven itself by the arrival V-infinity, which dictates the *inertial* velocity at EIP, and the selection of the approach hyperbola (B-angle).

Table 2. Proposed timeline for Operations at Mars between MAV ascent and TEI

Phase	Events	Duration	Time
MAV ascent			T_0
Orbit Matching (OM)	OS detection	14 days	$T_0 + 14$ d
	Hohmann transfer (*Homing*)	2 days	$T_0 + 16$ d
Rendezvous and capture	Co-elliptic approach / Far RdV (120 km to 5 km)	2 days	$T_0 + 18$ d
	Final approach / Close RdV (5 km to 100 m)	2 days	$T_0 + 20$ d
	Forced translation, OS capture and bio-sealing	2 days	$T_0 + 22$ d
Departure Orbit Acquisition (DOA)	Absolute RAAN phasing (assuming 200 deg)	24 days	$T_0 + 46$ d
	Apocentre raising to 4 sols	14 days	$T_0 + 60$ d
TEI			$T_0 + 60$ d

(points) and re-entry arcs[7] on an LST (Local Solar Time, X-axis), latitude (Y-axis) map, allowing to identify whether a target landing site is reachable and for which solar time. The right plot shows the corresponding values of the relative velocity at EIP, which exhibit a symmetry around the *inertial* velocity at EIP, represented by the central vertical line. On this plot, prograde entries appear on the left (lower atmospheric velocity), while retrograde entries (higher atmospheric velocity) appear on the right of that line.

Table 3 provides the main results for this example: both Utah and Woomera landing sites are accessible, however Utah can only be reached during daytime. However for different interplanetary transfers, and in particular arrival declinations, some landing sites can be excluded. Several arrival cases with a high approach declination have been found to be incompatible with a landing in Woomera, unless using an unrealistically steep re-entry (and near polar approach). A similar analysis has been carried out for all candidate transfers of interest for the architecture assessment.

7. ARCHITECTURE ASSESSMENT OVERVIEW

Based on the outcomes of the mission analysis, a number of mission architectures have been investigated, including purely chemical as well as hybrid (CP and EP stages) options. The four most promising have been down selected for further analysis, including preliminary spacecraft architecture. This assessment is beyond the scope of the paper and has been presented at the Second International Mars Sample Return Conference[1] in April 2018. The high-level conclusions are summarised by the diagram below: it has been found that the target return date of the samples was incompatible with the current assumptions for the baseline Launch Vehicle performance and payload mass.

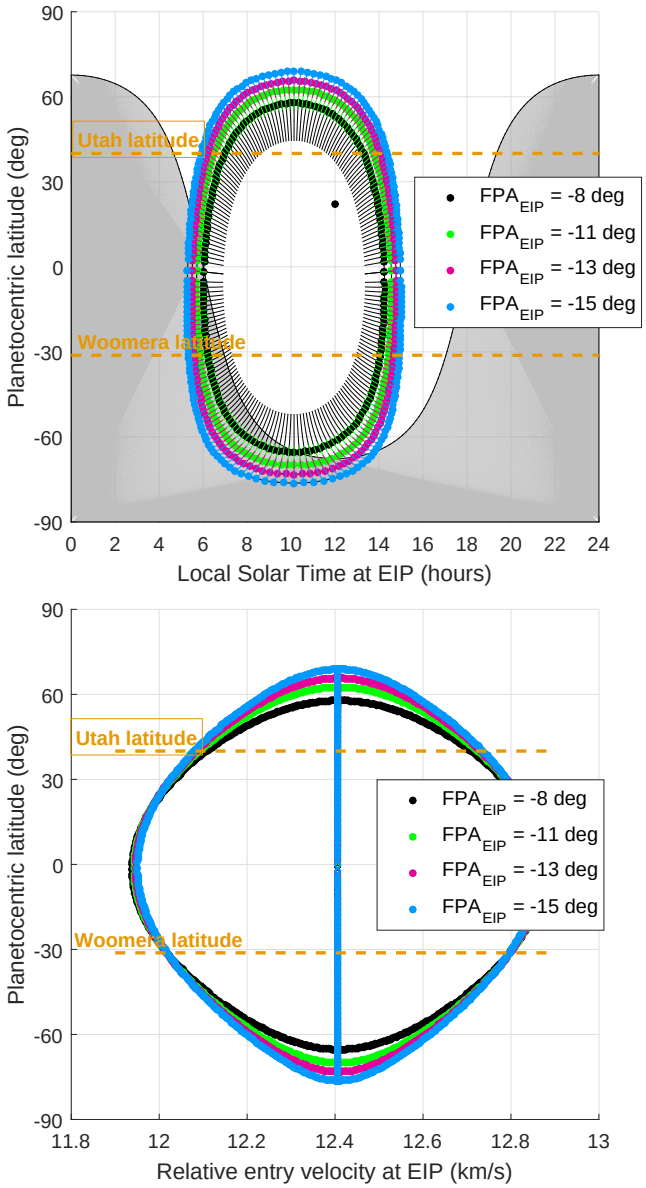

Fig. 16. Earth re-entry maps (top: LST/latitude, bottom: velocity/latitude) for the same transfer

[7]Re-entry arcs are propagated in a simple Keplerian model, from EIP to impact or from EIP to pericentre if the pericentre has a positive geocentric altitude.

Table 3. 2028-T1 CP Mars-Earth transfer - Re-entry conditions summary

Case (FPA angle)	EIP osculating perigee altitude (km)	Re-entry site	Relative velocity at EIP (km/s)	LST at EIP (hrs)
FPA = -13 deg	-155 km	Utah prograde	12.09	6.2
		Utah retrograde	12.73	14.1
		Woomera prograde	12.02	5.6
		Woomera retrograde	12.80	14.7
FPA = -11 deg	-78 km	Utah prograde	12.09	6.4
		Utah retrograde	12.72	13.8
		Woomera prograde	12.02	5.8
		Woomera retrograde	12.80	14.4
FPA = -8 deg	+15 km	Utah prograde	12.11	7.0
		Utah retrograde	12.71	13.3
		Woomera prograde	12.02	6.2
		Woomera retrograde	12.80	14.0

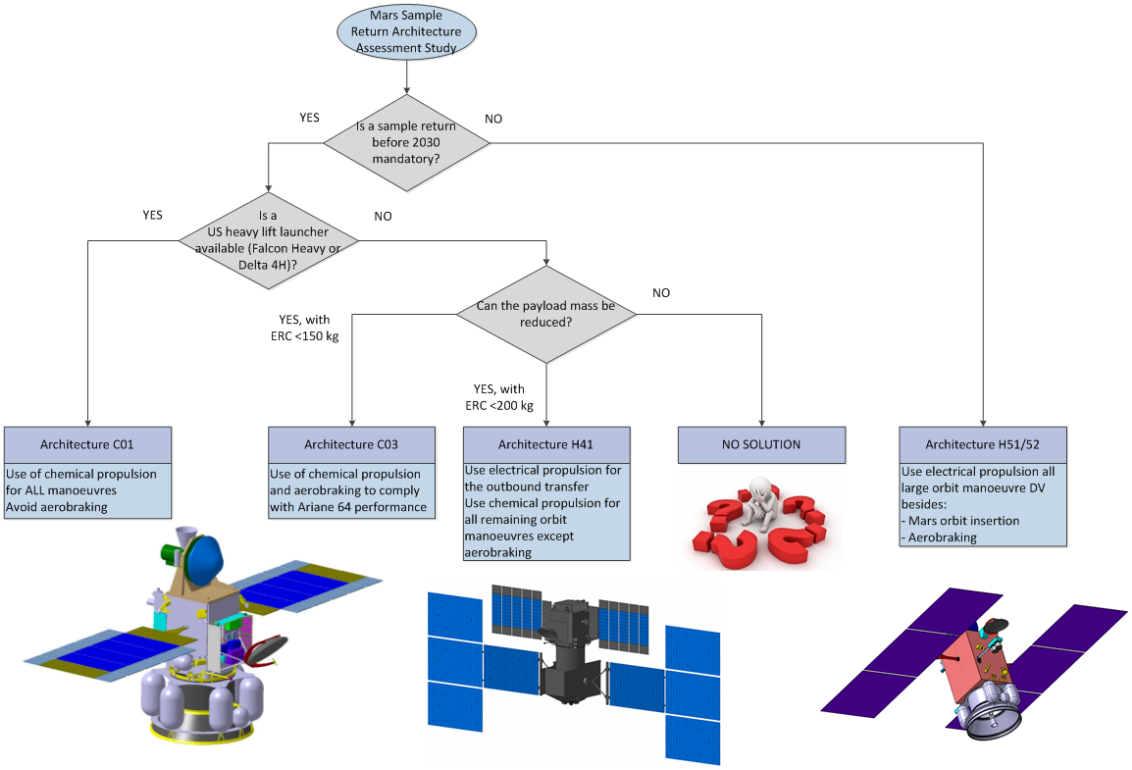

Fig. 17. Architecture assessment conclusion

8. CONCLUSION AND FUTURE WORK

This paper presented the mission analysis activities carried out in the frame of the *Mars Sample Return Architecture Assessment Study* (MSR-AA) conducted by Airbus for ESA in 2017. These activities covered all phases of the ERO mission in order to inform the main spacecraft and mission architecture trade-offs, including interplanetary CP and EP transfers, operations at Mars including aerobraking, communications with the lander and rendezvous, up until the Earth re-entry.

In 2018, Airbus has been awarded the *Mars Sample Return Earth Return Orbiter* (MSR-ERO) Phase A/B1 study by the European Space Agency, and thus given the opportunity to pursue its contribution to the MSR campaign, working in close collaboration with ESA and NASA JPL. While this system study will primarily focus on the spacecraft design itself, there still are a number of mission analysis and architecture trade-offs currently ongoing, looking at alternative CP transfer options in the case of the back-up mission (relaxed timeline returning long after 2030), also considering much higher power levels for some EP architectures leading to increased benefits from EP, in particular at Mars for the rendezvous, apocentre lowering (spiral-in) and orbit raising (spiral-out).

The Phase A will continue until the end of 2018, aiming at a preliminary design that shall then be further detailed and consolidated during the Phase B1, with the objective to reach the maturity level required to prepare a mission implementation proposal for the Ministerial Council at the end of 2019 (CM19).

9. ACKNOWLEDGEMENT

The Airbus authors are thankful to the ESA and JPL teams for their continued support during the MSR-AA study, the ongoing Phase A/B1, and their contributions to the paper. The first author is also particularly grateful to Steve Kemble, Senior Expert in Mission Analysis recently retired from Airbus after an inspiring career, for his extensive guidance and invaluable mentorship.

Notation

a	Semi-major axis
β	Solar β angle (between the orbital plane and the Sun vector)
e	Eccentricity
δ	Declination
ϵ	Axial tilt (or obliquity)
Ls	Areocentric solar longitude
ω	Argument of pericentre
Ω	Right Ascension of the Ascending Node (RAAN)

10. REFERENCES

[1] U. Derz, E. Joffre, M.-C. Perkinson, J. Huesing, F. Beyer, and J. M. Sanchez Perez, "Mars Sample Return Orbiter Architecture Options - Results of the ESA Mars Sample Return Architecture Assessment Study," in *Second International Mars Sample Return*, Apr. 2018, vol. 2071 of *LPI Contributions*, p. 6015.

Acronyms

A/B	Aerobraking
AoP	Argument of Pericentre
AU	Astronomical Unit (1 au = 149597870700 m)
CP	Chemical Propulsion
DLA	Declination of the Launch Asymptote
DOA	Departure Orbit Acquisition
DSM	Deep Space Manoeuvre
EDL	Entry, Descent & Landing
EGA	Earth Gravity Assist
EIP	Entry Interface Point
EP	Electric Propulsion
ERC	Earth Re-entry Capsule
ERO	Earth Return Orbiter
FPA	Flight Path Angle
HEO	High Elliptical Orbit
LMO	Low Mars Orbit
LST	Local Solar Time
MAV	Mars Ascent Vehicle
MOI	Mars Orbit Insertion
MSR	Mars Sample Return
NAC	Narrow Angle Camera
OD	Orbit Determination
OS	Orbiting Sample
RA/RAAN	Right Ascension / Right Ascension of the Ascending Node
RF	Radio Frequency
SRL	Sample Return Lander
TEI	Trans-Earth Injection
TOA	Target Orbit Acquisition